Molecular Biology of the Cell
Vol. 20, 3608–3616, August 1, 2009

CSN-5, a Component of the COP9 Signalosome Complex, Regulates the Levels of UNC-96 and UNC-98, Two Components of M-lines in *Caenorhabditis elegans* Muscle

Rachel K. Miller,*†‡§ Hiroshi Qadota,*§ Thomas J. Stark,*‖ Kristina B. Mercer,*¶ Tesheka S. Wortham,*† Akwasi Anyanful,* and Guy M. Benian*

*Department of Pathology and †Graduate Division of Biological and Biomedical Sciences, Emory University, Atlanta, GA 30322

Submitted March 13, 2009; Revised June 4, 2009; Accepted June 5, 2009
Monitoring Editor: William P. Tansey

In *Caenorhabditis elegans* two M-line proteins, UNC-98 and UNC-96, are involved in myofibril assembly and/or maintenance, especially myosin thick filaments. We found that CSN-5, a component of the COP9 signalosome complex, binds to UNC-98 and -96 using the yeast two-hybrid method. These interactions were confirmed by biochemical methods. The CSN-5 protein contains a Mov34 domain. Although one other COP9 signalosome component, CSN-6, also has a Mov34 domain, CSN-6 did not interact with UNC-98 or -96. Anti-CSN-5 antibody colocalized with paramyosin at A-bands in wild type and colocalized with abnormal accumulations of paramyosin found in *unc-98*, *-96*, and *-15* (encodes paramyosin) mutants. Double knockdown of *csn-5* and *-6* could slightly suppress the *unc-96* mutant phenotype. In the double knockdown of *csn-5* and *-6*, the levels of UNC-98 protein were increased and the levels of UNC-96 protein levels were slightly reduced, suggesting that CSN-5 promotes the degradation of UNC-98 and that CSN-5 stabilizes UNC-96. In *unc-15* and *unc-96* mutants, CSN-5 protein was reduced, implying the existence of feed back regulation from myofibril proteins to CSN-5 protein levels. Taken together, we found that CSN-5 functions in muscle cells to regulate UNC-98 and -96, two M-line proteins.

INTRODUCTION

Caenorhabditis elegans is an excellent model system in which to study muscle because of its optical transparency and powerful genetic tools available (Waterston, 1988; Moerman and Fire, 1997; Moerman and Williams, 2006). The muscle used for locomotion is located in the body wall and consists of 95 spindle-shaped mononuclear cells arranged in interlocking pairs that run the length of the animal in four quadrants. The myofibrils are restricted to a narrow ~1.5-μm zone adjacent to the cell membrane along the outer side of the muscle cell. The thin filaments are attached to the dense bodies (Z-disk analogs), and the thick filaments are organized around M-lines. All the dense bodies and M-lines are anchored to the muscle cell membrane and extracellular matrix, which is attached to the hypodermis and cuticle. This allows the force of muscle contraction to be transmitted directly to the cuticle and allows movement of the whole animal. Thus, worm muscle M-lines and dense bodies serve the function of analogous structures in vertebrate muscle. But, in addition, because of their membrane anchorage and protein composition (see for example, Qadota *et al.*, 2007), they are also similar to costameres of vertebrate muscle and focal adhesions of nonmuscle cells.

Over the last few years, multiple protein complexes have been found that link the muscle cell membrane to thick filaments at the M-line in *C. elegans*. The cytoplasmic tail of β-integrin is associated with a conserved four-protein complex that includes UNC-97 (PINCH in mammals; Mackinnon *et al.*, 2002; Lin *et al.*, 2003; Norman *et al.*, 2007). UNC-97, in turn, has been found to interact with one or two additional proteins linked or bound to myosin in the thick filaments (Miller *et al.*, 2006; Qadota *et al.*, 2007). Among the myosin-interacting proteins are UNC-98 and -96. These proteins were first identified by isolation of their loss-of-function mutants (Zengel and Epstein, 1980). Mutants of each gene have a similar and characteristic phenotype: by polarized light microscopy, each shows a disorganization of myofibrils and birefringent needles at the ends of the muscle cells. Molecular cloning revealed that each of these genes encode fairly small polypeptides of 300–400 residues. UNC-98 contains four C2H2 Zn fingers (Mercer *et al.*, 2003), but UNC-96 has no recognizable domains (Mercer *et al.*, 2006). Antibodies to each localize them to the M-lines. There is genetic and biochemical evidence that UNC-98 and -96 interact with each other (Mercer *et al.*, 2006) and with paramyosin (Mercer *et al.*, 2006; Miller *et al.*, 2008), an invertebrate-specific protein located in the cores of thick filaments, encoded by the gene *unc-15*.

This article was published online ahead of print in *MBC in Press* (http://www.molbiolcell.org/cgi/doi/10.1091/mbc.E09–03–0208) on June 17, 2009.

§ These authors contributed equally to this work.

Present addresses: ‡Department of Biochemistry and Molecular Biology, University of Texas M.D. Anderson Cancer Center, Houston, TX 77030; ‖Division of Biological Sciences, University of California, San Diego, La Jolla, CA 92093; ¶Department of Human Genetics, Emory University, Atlanta, GA 30322.

Address correspondence to: Guy M. Benian (pathgb@emory.edu).

Abbreviations used: ECL, enhanced chemiluminescence; HA, hemagglutinin; MBP, maltose-binding protein.

Interestingly, *unc-96* mutants contain discrete accumulations of UNC-98 protein, and *unc-98* mutants contain discrete accumulations of UNC-96 protein (Mercer *et al.*, 2006). These accumulations very likely correspond to the birefringent needles visualized by polarized light. In addition, both *unc-98* and *-96* mutants contain discrete accumulations of paramyosin. Both UNC-96 and -98 have diffuse localization within muscle of a paramyosin (*unc-15*) null mutant and show colocalization with paramyosin paracrystals in a paramyosin missense mutant (Miller *et al.*, 2008). By Western blot, in the absence of paramyosin, UNC-98 is diminished, whereas in paramyosin missense mutants, UNC-98 is increased. By yeast two-hybrid assay and ELISAs using purified proteins, UNC-98 interacts with paramyosin residues 31-693, whereas UNC-96 interacts with a separate region of paramyosin, residues 699-798. Paramyosin lacking the C-terminal UNC-96–binding region fails to localize throughout the A-bands. This data are compatible with a model we proposed in which UNC-98 and -96 may act as chaperones to promote the incorporation of paramyosin into thick filaments (Miller *et al.*, 2008). To gain insight into the function of UNC-98 and -96, we have been identifying and learning the functions of their binding partners initially through a two-hybrid approach followed by confirmation by biochemical assays and interpretation using mutations and RNA interference (RNAi). Here we report that, unexpectedly, both UNC-98 and -96 interact with CSN-5, a component of the evolutionarily conserved COP9 signalosome, which has been implicated in a wide variety of biological functions usually linked to ubiquitin-mediated proteolysis. Our results are the first to implicate CSN-5 or the COP9 signalosome in myofibrillar organization or function.

MATERIALS AND METHODS

Nematode Strains and Culture

The following *C. elegans* strains were used in these studies: wild-type N2, *unc-96 (sf18)*, *unc-98 (sf19)*, *unc-15 (e1215)*, *unc-15 (e1214)*, and *unc-15 (e73)*. Nematodes were grown at 20°C on NGM agar plates with *Escherichia coli* strain OP50 (Brenner, 1974).

Yeast Two-Hybrid Screens and Assays

The general methods used for screening a *C. elegans* cDNA yeast two-hybrid library were described in Miller *et al.* (2006). The bait region for UNC-98 included residues 1-112 (Miller *et al.*, 2006) and for UNC-96, residues 201-418 (Mercer *et al.*, 2006). To construct a prey plasmid that contained residues 1-165 of CSN-5, PCR was used to produce from a cDNA pool the corresponding cDNA using the 5′ primer GACT GGATCCATGGAAGTTGATAACGTCAAGC with an added BamHI site and the 3′ primer AGTC GTCGACTGGCTCTTGGAACTTTTGATTG with an added SalI site. After insertion into pGAD-C1 a clone was identified without errors. To make a prey plasmid that contained residues 166-369 of CSN-5, PCR was used to produce a cDNA using the 5′ primer GACTGGATCCTGGGTTGCTATTGTTATTGATC with a BamHI site and the 3′ primer AGTCGTCGACTTAAGCATCGGCCATCTCAAC with a SalI site, insertion into pBluescript, finding an error-free clone and finally moving the same fragment into pGAD-C1. To construct full-length *csn-6* prey plasmid, first PCR was used to amplify a full-length cDNA from a cDNA pool using the 5′ primer CGCGGATCCATGGCATTGAACGCACCAAGC with an added BamHI site and the 3′ primer CGCGGTCGACTTATGAAGCTTGACTCGACTC with an added SalI site; the resulting fragment was cloned into pBluescript, and after identifying an error-free clone, the fragment was excised using BamHI and SalI and inserted into the two-hybrid prey vector pGAD-C1. Yeast two-hybrid assays were performed as described in Mackinnon *et al.* (2002).

Yeast and Bacterial Expression of Fusion Proteins

To prepare the yeast-expressed, hemagglutinin (HA)-tagged, full-length CSN-5 (HA-CSN-5), cDNA was PCR amplified using the 5′ primer CGATCGCCCGGGATGGAAGTTGATAACGTCAAG with an added SmaI site, and the 3′ primer GATCCTCGAGTTAAGCATCGGCCATCTCAAC with an added XhoI site. This fragment was inserted between the EcoRV and SalI sites of the vector pKS-HA8(Nhex2). After finding an error-free clone, the NheI fragment was cloned into pGAP-C-Nhe (yeast expression vector, TRP1 marker) by using the NheI site of the vector. The resulting plasmid was transformed into yeast strain PJ69-4A. Conditions for yeast growth, preparation of a lysate, and immunoprecipitation of HA-CSN-5 were as described in Qadota *et al.* (2008).

Preparation of bacterially expressed maltose-binding protein (MBP)-UNC-96 (201-418) has been described in Mercer *et al.* (2006). To prepare bacterially expressed MBP-UNC-98 (1-112), the BamHI-SalI fragment from pGBDU-4c (Mercer *et al.*, 2003) was inserted into pMAL-KK-1. To prepare bacterially expressed full-length CSN-5 with a C-terminal 6His tag, cDNA was PCR amplified using the 5′ primer GTACGGATCCATGGAAGTTGATAACGTCAAGC with an added BamHI site, and the 3′ primer GATCCTCGAGAGCATCGGCCATCTCAACAGC with an added XhoI site. The fragment was inserted between BamHI and XhoI sites in pET24a. After finding an error-free clone by sequencing, the plasmid was transformed into BL21 codon plus (DE3) RIL competent cells (Stratagene, La Jolla, CA). Expression and purification of CSN-5-His was accomplished by using the His-Bind column system (Novagen/EMD Biosciences, Madison, WI).

HA Pulldown Assay

The method for trying to determine whether yeast expressed HA-CSN-5 (full length) interacts with bacterially expressed MBP-UNC-96 (201-418) or MBP-UNC-98 (1-112) was described in Qadota *et al.* (2008).

Far Western Assay

A far Western assay for determining if bacterially expressed CSN-5-6His interacts with bacterially expressed MBP-UNC-96 (201-418) or MBP-UNC-98 (1-112) was performed essentially as described in Mercer *et al.* (2006).

Generation of Anti-CSN-5 Antibodies

The C-terminal 202 residues of CSN-5 (aa 167-369) were expressed and purified in *E. coli* as an MBP fusion protein. To do this primers, GACTGGATCCTGGGTTGCTATTGTTATTGATC for the 5′ end (with added BamHI site) and AGTCGTCGACTTAAGCATCGGCCATCTCAAC for the 3′ end (with added SalI site) were used to create a PCR fragment from a cDNA pool and cloned into Bluescript. After finding an error-free clone, the fragment was excised, cloned into pMAL-KK1 using the same restriction sites, and used for protein expression as described in Mercer *et al.* (2006). The resulting MBP-CSN-5 (167-369) was shipped to Spring Valley Laboratories (Woodbine, MD) for generation of rabbit polyclonal antibodies. After removal of most of the anti-MBP antibodies by immunoprecipitation with MBP-UNC-96 (201-418) (Mercer *et al.*, 2006), anti-CSN-5 antibodies were affinity-purified against MBP-CSN-5 as described previously (Mercer *et al.*, 2003).

Western Blots and Immunofluorescence Localization of Proteins

We used the procedure of Hannak *et al.* (2002) to prepare total protein lysates from wild-type, *unc-96*, *-98*, and *-15* mutant worms and from *rrf-3(pk1426)* RNAi hypersensitive worms (Simmer *et al.*, 2002) subjected to RNAi by feeding with empty vector, or for *csn-5*, *-6*, or both *csn-5* and *-6* (see below). When comparing wild type and mutants, or empty vector and RNAi for various genes, we loaded approximately equal total amounts of protein extract estimated by finding volumes of extracts that would give equal intensity of banding after Coomassie staining. To assure that equal total protein was loaded per lane, using Western blotting, we compared the amount of actin or paramyosin present. We used quantities of extracts and dilutions of antibodies that would place us into the linear range of detection by enhanced chemiluminescence (ECL) and exposure to film. For detection of UNC-98, we used anti-UNC-98 affinity purified to the N-terminal residues 1-112 as described in Miller *et al.* (2006) at 1:200 dilution. Affinity-purified antibodies to UNC-96 (Mercer *et al.*, 2006) and to CSN-5 were also used at 1:200 dilutions. Monoclonal antibodies to actin (clone C4; Chemicon International, Temecula, CA) were used at 1:12,000 dilution, and antibodies to paramyosin (5-23; Miller *et al.*, 1983) were used at 1:2000 dilution. The quantitation of UNC-98 protein levels shown in Figure 8B was performed on a representative Western blot, using Adobe Photoshop (San Jose, CA) and a method described in the following Web site: https://www.lukemiller.org/journal/2007/08/quantifying-Western-blots-without.html. For each lane, the UNC-98 level was normalized to that of actin. The relative amount of UNC-98 protein for each RNAi experiment, was expressed as follows: (experimental value/empty vector value) × 100.

For immunostaining, adult worms were fixed as described in Nonet *et al.* (1993). Anti-CSN-5 (see above) was used at 1:100 dilution, anti-α-actinin (monoclonal MH35; Francis and Waterston, 1985) at 1:200 dilution, anti-paramyosin (monoclonal 5-23; Miller *et al.*, 1983) at 1:200 dilution, and anti-myosin heavy chain A (MHC A; monoclonal 5-6; Miller *et al.*, 1983) at 1:200 dilution. Secondary antibodies and confocal microscopy were as described in Qadota *et al.*, 2007.

RNAi for csn-5 and -6

RNAi was performed by a feeding method (Simmer *et al.*, 2002). The following plasmids were used: pPD129.36-csn-5 for *csn-5*, pPD129.36-csn-6 for *csn-6*, and pPD129.36-csn-5/-6 for *csn-5* and *-6* double RNAi. To construct pPD129.36-csn-5, the XhoI fragment of 4c-4-2 (originally isolated from yeast two-hybrid screening with UNC-98 N-terminus as bait (Miller *et al.*, 2006), containing full-length *csn-5* cDNA) was cloned into the XhoI site of pPD129.36 (Timmons *et al.*, 2001). pPD129.36-csn-6 was made by insertion of PCR-amplified *csn-6* full-length cDNA into pPD129.36 between BamHI and XhoI sites. For making the pPD129.36-csn-5/-6 plasmid, the XhoI fragment of 4c-4-2 was cloned into the XhoI site of pPD129.36-csn-6.

For immunostaining of RNAi worms, the following method was used. Feeding bacteria containing the RNAi plasmids noted above were cultured in liquid 2xYT and induced using a final concentration of 0.4 mM IPTG for 4 h. Liquid culture of induced cells was spotted onto NGM plates containing ampicillin (50 μg/ml) and tetracycline (15 μg/ml). Worms were picked onto five 6-cm RNAi plates (each containing three spots of induced bacteria) at 10 worms per plate, and these plates were incubated at 20°C overnight to eliminate RNAi nonaffected eggs. The next day, the 10 worms were transferred from the five 6-cm plates to five 10-cm plates (each containing 11 spots of induced bacteria) and incubated at 20°C for 8 h for these animals to lay F1 generation eggs. After 8 h, the 10 parental worms were removed from each of the 10-cm plates. After 3-d incubation at 20°C, the F1 generation attained young adulthood, a good stage for immunostaining using the method of Nonet *et al.* (1993).

For the preparation of Western blot lysates or total RNA (see below), the following method was used. Worms were picked onto 25 6-cm RNAi plates (each containing three spots of induced bacteria) at 10 worms per plate, and these plates were incubated at 20°C overnight to eliminate RNAi nonaffected eggs. The next day, the 10 worms were transferred from the 25 6-cm plates to 25 10-cm plates (each containing 11 spots of induced bacteria) and incubated at 20°C for 8 h for these animals to lay F1 generation eggs. After 8 h, the 10 parental worms were removed from each of the 10-cm plates. After 3-d incubation at 20°C, the F1 generation attained young adulthood, and the worms were collected from the plates by washing them off with M9 buffer.

Real-Time PCR Assays

Total RNA from approximately ~100–200-μl pellets of F1 worms (described above) that had been fed bacteria containing either *csn-5* RNAi or empty vector was extracted using Trizol (Invitrogen, Carlsbad, CA) using the manufacturer's procedure and quantitated by UV absorbance. First-strand cDNAs were synthesized with random decamers using a RETROscript kit (Applied Biosystems, Foster City, CA). The following primers were used to amplify ~120-base pair cDNAs from *unc-98* and *ges-1*: Q982F: TTTGGATGGCAGTGATCAACAGG, Q982R: GAGTGTTCATGAAGTTGAATGTGAG, ges-1F: CACTCCTCACTATCGTTTAGTC, and ges-1R: CGTGAATCCAGAACAGAACTG. Standard PCR using these primers and first-strand cDNAs revealed contamination of the RNA with genomic DNA. Therefore, the RNA samples were treated with RNase-free DNAse (TURBO DNA-free from Applied Biosystems), the first-strand cDNAs were made again, and agarose gel analysis of trial PCRs revealed production of the single bands of expected size without genomic DNA contamination. Real-time PCR was performed in 50-μl volumes using SYBR-green detection in a 96-well plate on an iCycler machine (Bio-Rad, Hercules, CA). Three independent reactions were performed in duplicate from each of two independently generated first-strand cDNAs for each sample (empty vector or *csn-5 (RNAi)*). The PCR reactions were initiated at 95°C for 4 min followed by 40 cycles of, 15 s at 95°C, 60 s at 60°C, and 30 s at 68°C using Platinum Taq DNA polymerase (Invitrogen). The following equation, adapted from Maeda *et al.* (2006), was used: % Δ in *unc-98* mRNA = $2^{(\text{Ct of } csn\text{-}5\ (RNAi)) - (\text{Ct of empty vector})} \times 100$, in which Ct of *csn-5 (RNAi)* = (average Ct value of *unc-98* mRNA − average Ct value of *ges-1* mRNA), and Ct of empty vector = (average Ct value of *unc-98* mRNA − average Ct value of *ges-1* mRNA).

Polarized Light Microscopy

Polarized light microscopy was performed as described previously (Mercer *et al.*, 2006).

RESULTS

CSN-5 Interacts with UNC-98 and -96

As reported previously (Miller *et al.*, 2006), when we used the N-terminal 112 residues of UNC-98 as bait to screen a yeast two-hybrid library of *C. elegans* cDNAs, preys representing 18 unique proteins were recovered. Among them were 10 clones representing full-length cDNA for *csn-5* (Supplemental Data in Miller *et al.*, 2006). Because of the similarity in mutant phenotype of *unc-98* and *-96*, their genetic interaction, their interaction as proteins, and their colocalization at the M-line (Mercer *et al.*, 2006), a similar screen was conducted with UNC-96. A bait representing the C-terminal half of UNC-96 yielded two independent clones for CSN-5. CSN-5 is the *C. elegans* ortholog of subunit 5 of the COP9 signalosome (CSN) complex conserved in plants and animals and functions in controlling protein degradation, either in stabilizing some proteins, or in promoting the degradation of other proteins (for reviews see Cope and Deshaies, 2003; Schwechheimer, 2004). In *C. elegans*, the COP9 signalosome contains five proteins with PCI domains and two proteins, CSN-5 and CSN-6, with Mov34 (also known as MPN) domains (Luke-Glaser *et al.*, 2007).

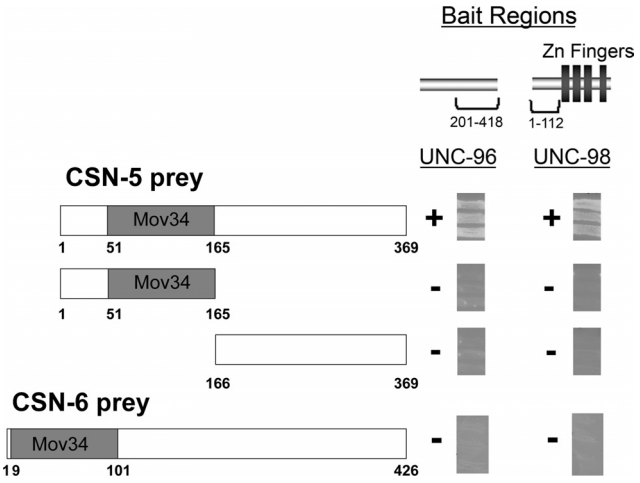

Figure 1. Yeast two-hybrid assays demonstrate the interaction between specific portions of UNC-96 or -98 with CSN-5. Top right, representation of the UNC-96 and -98 baits used. Left, representation of CSN-5 or -6 preys used. In each case, recognizable protein domains are indicated (C2H2 Zn fingers in UNC-98, Mov34 domains in CSN-5 and -6). Images of growth of three independent colonies of yeast on −Ade plates are shown and summarized as follows: +, growth and −, no growth. Note that interaction of the C-terminal half of UNC-96 or the N-terminal 112 residues of UNC-98 require full-length CSN-5. CSN-6, the other protein of the COP9 complex that contains a Mov34 domain, fails to interact with either UNC-96 or -98.

As shown in Figure 1, by two-hybrid analysis, interaction of the C-terminal half of UNC-96 or the N-terminal 112 residues of UNC-98 require full-length CSN-5. Neither residues 1-165, containing the Mov34 domain, nor residues 166-369 of CSN-5 alone are sufficient. In addition, the other Mov34 domain containing protein in *C. elegans*, CSN-6, failed to interact with either UNC-96 or -98 (Figure 1).

To verify the interactions identified by two-hybrid assay, two different biochemical assays were used with purified CSN-5, UNC-98, and -96 proteins. In the first assay, total protein extracts were prepared from yeast expressing HA-tagged CSN-5, immunoprecipitated with beads coated with antibodies to HA, washed, and incubated with purified, bacterially expressed MBP-UNC-98 (1-112), MBP-UNC-96 (201-418), or MBP, and then washed, and the bound proteins were eluted. As shown by the immunoblots in Figure 2A (top), each reaction contained equal amounts of purified HA-CSN-5, but only MBP-UNC-98 was copelleted. This verifies interaction between purified CSN-5 and purified UNC-98. In the second assay, far Western blot analysis was used. Bacterially expressed CSN-5 with a C-terminal 6His tag was purified, separated on a gel, and blotted, and then the blot was incubated with either MBP-UNC-98 (1-112), MBP-UNC-96 (201-418), or MBP. As shown in Figure 2B, reaction

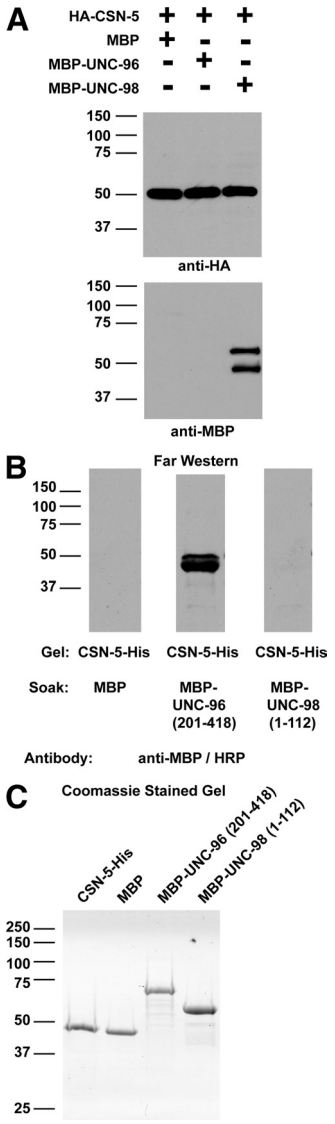

Figure 2. Verification of interaction between CSN-5 and either UNC-96 or -98. (A) Bacterially expressed MBP-UNC-96 (aa 201-418) and MBP-UNC-98 (1-112) interact with yeast expressed HA-CSN-5. Total protein extracts were prepared from yeast expressing HA-CSN-5, incubated with agarose beads coated with antibodies to HA, washed, and then incubated with purified, bacterially expressed MBP, MBP-UNC-96, or MBP-UNC-98, and washed; then the proteins were eluted, and portions of each sample were separated by SDS-PAGE in two gels (10%) and blotted. As shown on top, reaction of one blot with anti-HA shows that in each reaction, HA-CSN-5 is present. As shown on the bottom, reaction with anti-MBP reveals that MBP-UNC-98 was copelleted (top band, full-length product; bottom band, likely degradation product). (B) The C-terminal half of UNC-96 interacts with CSN-5 by far Western assay. SDS-PAGE was used to separate CSN-5-His, and the protein was transferred to a membrane. One blot strip was incubated with MBP, one blot strip was incubated with MBP-UNC-96 (201–418), and a third blot strip was incubated with MBP-UNC-98 (1–112). After washing, each blot strip was incubated with antibodies to MBP coupled to horseradish peroxidase (anti-MBP/HRP), and reactions visualized by ECL. (C) A Coomassie-stained 10% SDS-PAGE shows 2 μg of each bacterially expressed protein used in the far Western or HA pulldown. For each blot or gel, the positions of molecular-weight size markers in kDa are indicated.

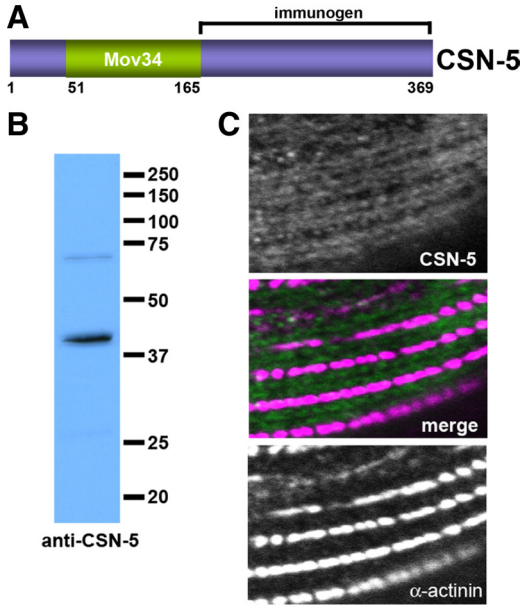

Figure 3. Antibodies raised to CSN-5 detect a polypeptide from worm extracts of expected size and localize to muscle A-bands. (A) Schematic of CSN-5 indicating that a nondomain containing region, residues 166-369, was used as immunogen to generate rabbit polyclonal antibodies. (B) Western blot of whole worm extracts from wild type reacted with affinity-purified antibodies to CSN-5. Major reaction is to an approximately 40-kDa polypeptide, the size expected from the CSN-5 sequence. Molecular-weight standards are shown at the right. (C) Anti-CSN-5 localize to A-bands in body wall muscle. Anti-CSN-5 and anti-α-actinin were coincubated with wild-type *C. elegans*, and the muscle was imaged by confocal immunofluorescence microscopy. The images show a portion of one body wall muscle cell. α-Actinin is a marker for dense bodies. Bar, 10 μm.

with antibodies to MBP revealed an interaction of CSN-5 with UNC-96. This verifies interaction between purified CSN-5 and purified UNC-96.

Anti-CSN-5 Localizes to Muscle A-Bands

As one way to determine if these interactions occur in vivo, we wanted to determine if and where CSN-5 is located in the sarcomere. We raised rabbit polyclonal antibodies to a region of CSN-5 outside the Mov34 domain to avoid possible cross-reaction with CSN-6 (Figure 3A). After affinity purification, these antibodies primarily react with a protein of ~40 kDa, the size expected from the CSN-5 sequence (Figure 3B). Further indication that this band represents the *csn-5* product was obtained when a Western blot was performed with an extract from *csn-5 (RNAi)* worms: this protein band was greatly diminished (see Figure 8). When these antibodies were used to stain adult worms, localization was observed in body wall muscle at A-bands in a pattern very similar to the localization of paramyosin (Figure 3C). Indeed, when wild-type worms were costained with anti-CSN-5 and a monoclonal to paramyosin, colocalization was seen (Figure 4, left column).

CSN-5 Colocalizes with Abnormal Accumulations of Paramyosin in unc-98, -96, and -15 Mutant Muscle

The hallmark of the *unc-96* or *-98* mutant body wall muscle is the presence birefringent "needles" at the ends of the muscle cells as observed by polarized light microscopy (Zengel and Epstein, 1980; Mercer *et al.*, 2003, 2006). These

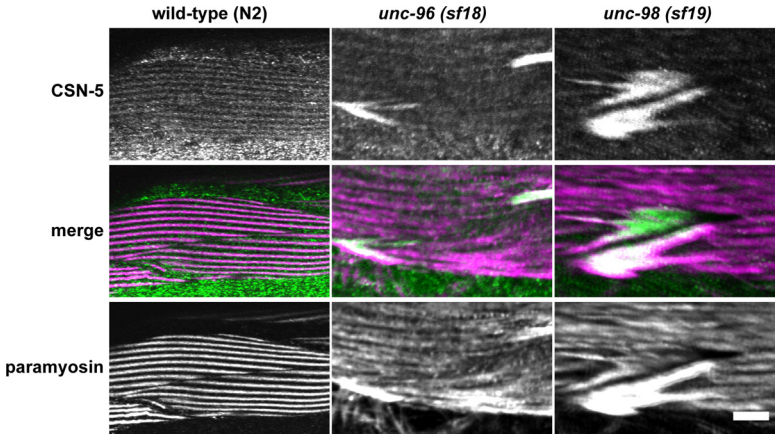

Figure 4. Immunofluorescence localization of CSN-5 and paramyosin in wild-type and in *unc-96 (sf18)* and *unc-98 (sf19)* mutant muscle. In wild-type muscle, CSN-5 localizes to A-bands, colocalizing with paramyosin. In both *unc-96* and *-98*, some CSN-5 is found in A-bands, but much of it is found in needle-like accumulations containing paramyosin at the ends of muscle cells. Bar, 10 μm.

needles likely contain accumulations of paramyosin in either *unc-96* or *-98* mutants, UNC-98 protein in *unc-96* mutants, and UNC-96 protein in *unc-98* mutants (Mercer *et al.*, 2006; Miller *et al.*, 2008). Thus, given the interaction between CSN-5 and UNC-96 and -98, we wanted to determine if CSN-5 was also present in the needles or paramyosin accumulations. When the anti-CSN-5 antibodies were used to stain *unc-96* and *-98* mutants, CSN-5 was found at both A-bands and in accumulations at the ends of the muscle cells, colocalizing with paramyosin (Figure 4). Additionally, we examined the localization of CSN-5 in an *unc-15* missense mutant, *e1215*, that contains paramyosin paracrystals. As shown in Figure 5, CSN-5 and paramyosin colocalize, including in the paramyosin paracrystals. Similarly, we had shown that these paramyosin paracrystals in *unc-15 (e1215)* also contain UNC-98 and -96 (Miller *et al.*, 2008). Thus, in three conditions (*unc-96*, *-98*, and *-15* mutants) in which abnormal accumulations or paracrystals of paramyosin are formed, CSN-5 is associated with the abnormal paramyosin.

RNAi Knockdown of csn-5 Increases the Level of UNC-98 Protein

Because CSN-5 localizes to the A-band, we wondered whether A-band organization would be disrupted when *csn-5* was reduced in activity. In addition, because CSN-5 and -6 each have a Mov34 domain and thus might have redundancy in function, we wondered whether A-band organization would be disrupted when *csn-6* was reduced in activity. Because intragenic deletions that are presumably null for *csn-5* are sterile (our unpublished observations), such strains would be inconvenient for protein localization studies. In addition, Smith *et al.* (2002) reported that RNAi for *csn-5* results in sterility with small gonads and lack of oocytes. Nevertheless, we could feed large numbers of wild-type worms bacteria producing *csn-5* double-strand RNA (dsRNA) and examine the muscle structure of the F1 adults. This was conducted for *csn-5*, *csn-6* and a double *csn-5 csn-6* RNAi construct. As shown in Figure 6, these treatments resulted in no defects in A-band organization, either in the localization of paramyosin, which is located in the polar

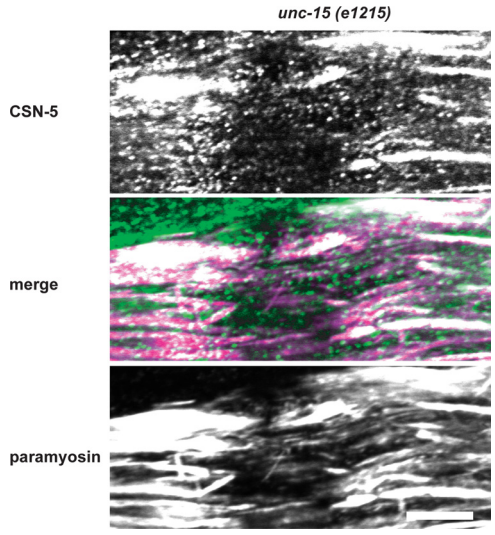

Figure 5. CSN-5 colocalizes with paramyosin in a paramyosin missense mutant. The paramyosin missense mutant, *unc-15 (e1215)*, has paramyosin paracrystals within its body wall muscle cells. These accumulations of paramyosin also contain CSN-5. Bar, 10 μm.

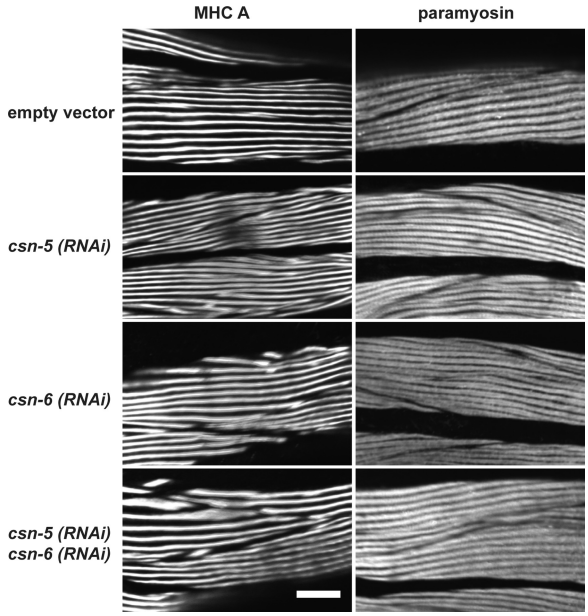

Figure 6. Knockdown of *csn-5*, *-6*, or both together has no effect on the localization of two thick filament components, MHC A and paramyosin. Wild-type worms were subjected to RNAi by feeding using either the empty vector or with vectors containing the indicated genes. F1 adults were fixed and immunostained with either anti-MHC A or anti-paramyosin. RNAi with the empty vector resulted in worms with the same staining pattern as unfed wild-type worms. Bar, 10 μm.

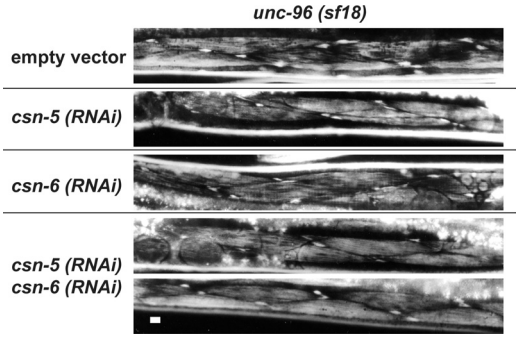

Figure 7. Knockdown of *csn-5* and *-6* together results in a mild improvement in myofibrillar structure of *unc-96 (sf18)* animals. Polarized light images of *unc-96 (sf18)* animals after RNAi by feeding of bacteria harboring either empty vector or with vectors containing the indicated genes. In the worms fed the empty vector note the typical appearance of *unc-96* mutant animals with myofilament of reduced organization and birefringent needles at the ends of the muscle cells. RNAi of either *csn-5* or *-6* alone has no effect on this appearance. However, double RNAi for *csn-5* and *-6* results in mild improvement, with better organized lattice and fewer or less intense needles (portions of two different animals are shown). Bar, 10 μm.

regions of the A-band, or myosin heavy chain A (MHC A), which is located in the middle of A-bands. Moreover, no needle-like accumulations of paramyosin were seen.

Because we had shown that CSN-5 interacts with UNC-96 and -98, we determined what would happen to the phenotype of *unc-96* or *-98* mutant worms when *csn-5* was knocked down by RNAi. As shown in Figure 7, the polarized light phenotype of *unc-96 (sf18)* mutant worms was not affected by either empty RNAi vector or *csn-5* or *-6* RNAi. However, in the *csn-5 csn-6* double RNAi, there was a mild improvement in the Unc-96 phenotype, especially in the organization of myofibrils. The fact that improvement in myofibril organization was only seen in the double RNAi is consistent with the Western data described below (Figure 8) in which the double RNAi more strongly knocked down the level of CSN-5 protein than either single RNAi. The analogous experiment yielded no changes in the phenotype of *unc-98 (sf19)* mutant worms (data not shown).

Because the COP9 signalosome is known in multiple organisms to regulate protein stability, we examined what effect reduction in CSN-5 would have on the protein levels of its two suspected interactors in muscle, UNC-96 and -98, and also paramyosin, which has been shown previously to interact with UNC-96 and -98 (Miller *et al.*, 2008). Protein extracts from F1 animals fed dsRNA for *csn-5*, *-6,* and the *csn-5 csn-6* double, were examined by quantitative Western blotting. As shown in Figure 8A, RNAi was effective in reducing the levels of CSN-5 in *csn-5 (RNAi)* and *csn-5 csn-6* double RNAi animals, as expected. Somewhat surprisingly, CSN-5 levels were also reduced in *csn-6 (RNAi),* although this result is compatible with the observation of Pintard *et al.* (2003) that at least by two-hybrid assay, *C. elegans* CSN-5 and -6 interact. Also, it is not likely that our anti-CSN-5 antibodies cross-react with CSN-6 given that the immunogen used has no homology to CSN-6 and the sizes of the expected proteins are different (40.6 kDa for CSN-5 and 46.9 kDa for CSN-6). Although our RNAi treatments had no effect on the levels of paramyosin or actin, when *csn-5* was knocked down by either *csn-5 (RNAi)* or *csn-5 csn-6 (RNAi),* there was an increase in the level of UNC-98 protein. Quantitation of UNC-98 levels of the representative Western blot experiment shown in Figure 8A was performed using actin levels as loading controls and the results are depicted in Figure 8B. As compared with animals fed bacteria carrying the empty RNAi vector, *csn-5 (RNAi)* and *csn-5 (RNAi) csn-6 (RNAi),* resulted in 2.1- and 2.7-fold higher levels of UNC-98 protein, respectively. Because nematode CSN-5 has been shown by antibody staining to reside in both cytoplasm and nuclei of most cell types (Smith *et al.,* 2002; Pintard *et al.,* 2003), we wondered if *csn-5* knockdown might affect *unc-98* transcription. This was investigated by performing quantitative real-time RT-PCR for *unc-98* mRNA in worms fed RNAi empty vector versus *csn-5 (RNAi).* We normalized the *unc-98* mRNA levels to those of *ges-1* mRNA, which encodes a carboxylesterase expressed specifically in the gut (Aamodt *et al.,* 1991). As shown in Figure 8C, knockdown of *csn-5* resulted in a 1.3-fold increase in *unc-98* mRNA. Because the increase in UNC-98 protein is greater than that in *unc-98* mRNA (2.1- vs. 1.3-fold), the increase of *unc-98* mRNA might not be the main reason for the increase in UNC-98 protein caused by *csn-5* knockdown. Our results are at least consistent with a normal role of CSN-5 in promoting the degradation of UNC-98 protein (see *Discussion*). Finally, as shown in Figure 8A, the effects on protein levels of UNC-96 were not so obvious although there was a mild decrease of UNC-96 when *csn-5*, *-6,* or especially both *csn-5* and *csn-6* were knocked down. Thus, this result would be consistent with a normal role of CSN-5 in promoting the stability of UNC-96.

Loss-of-Function Mutations in unc-96 and -15 Result in Diminished Levels of CSN-5 Protein

We also wanted to determine whether the levels of CSN-5 might be affected by the levels of UNC-96, -98, or the level or state of paramyosin. As shown in Figure 9A, and as shown previously (Miller *et al.,* 2008), the levels of paramyosin are similar in wild-type, *unc-96,* and *-98* loss-of-function mutant animals. However, in *unc-96* mutants (but not *unc-98* mutants), the level of CSN-5 is significantly diminished. As shown in Figure 9B, the level of CSN-5 was examined in three mutant alleles of *unc-15* (paramyosin): in the null allele, *e1214,* and in the missense alleles *e1215* and *e73,* each of which form paramyosin paracrystals. In the absence of paramyosin (*e1214*), CSN-5 is significantly diminished. (Similarly, in the absence of paramyosin, UNC-98 is diminished; Miller *et al.,* 2008.) In the presence of abnormal paramyosin, *e73* and to some extent *e1215*, moderate decreases in the levels of CSN-5 were also observed. (In contrast, in the presence of these abnormal paramyosins, UNC-98 levels were increased; Miller *et al.,* 2008).

DISCUSSION

In summary, we have identified an interaction between the highly conserved COP9 signalosome component CSN-5, implicated in control of protein levels, with two known components of nematode sarcomeric M-lines: UNC-98 and -96. CSN-5 was found to colocalize with paramyosin in wild-type muscle and to colocalize with abnormal aggregates of paramyosin in *unc-96* and *unc-98* loss-of-function mutants and in paramyosin (*unc-15*) missense mutants. RNAi knockdown of *csn-5* together with the similar protein *csn-6* did not result in a defect in myofibrillar structure, but it did result in a mild improvement in the muscle structure of *unc-96* mutant muscle.

We have obtained insight into the meaning of direct interaction between CSN-5 and UNC-98 and -96 from the Western blot experiments (Figure 8). In *csn-5 (RNAi)* and *csn-5 csn-6* double RNAi animals, the amount of UNC-98

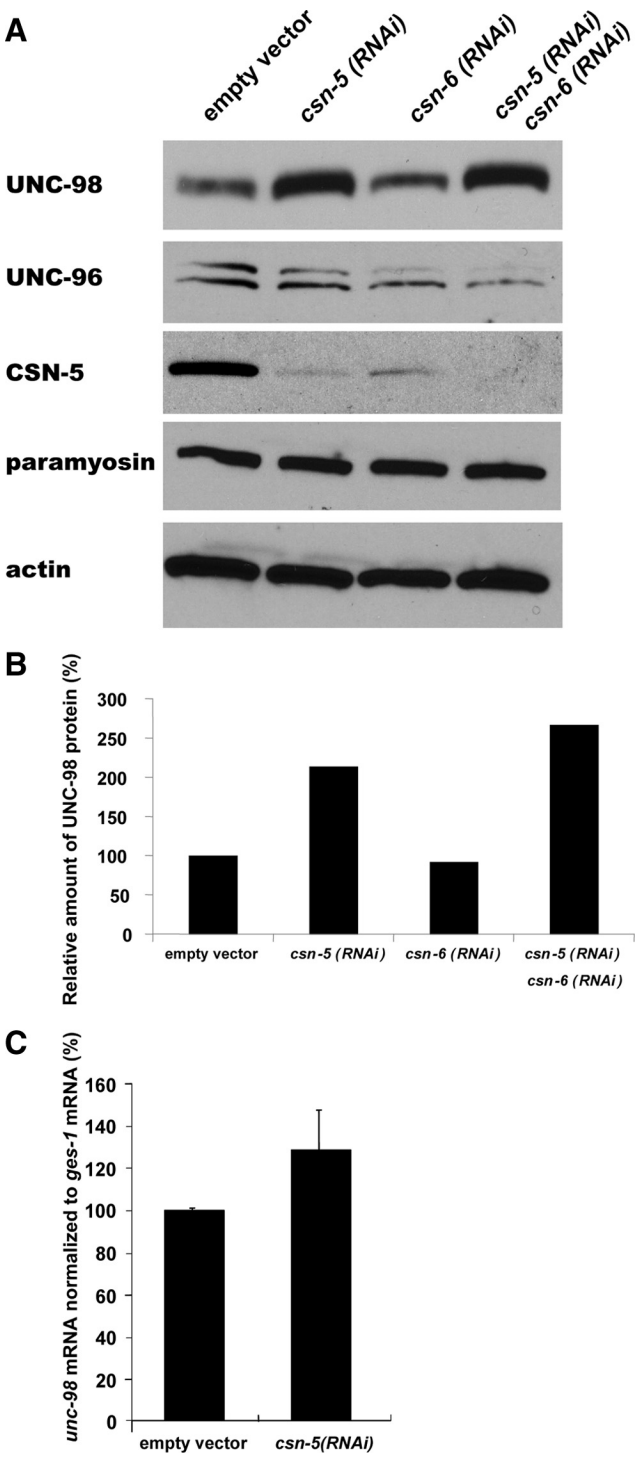

Figure 8. RNAi for *csn-5* results in an increase in the levels of UNC-98 protein. (A) Extracts containing equal amounts of total Laemmli-soluble proteins from F1 progeny of animals fed either the RNAi by feeding empty vector or vectors containing *csn-5* or *-6* or both *csn-5* and *-6*, were separated on a gel, blotted, and reacted with antibodies to the indicated proteins. As expected, the level of CSN-5 is reduced in *csn-5 (RNAi)* or in *csn-5 (RNAi) csn-6 (RNAi)*. Unexpectedly, CSN-5 is also reduced in *csn-6 (RNAi)*. Note that when *csn-5* was knocked down, the level of UNC-98 was increased. The levels of actin and paramyosin served as loading controls. (B) Quantitation of UNC-98 protein levels under different conditions. For each lane, the UNC-98 level was normalized to that of actin. As compared with empty RNAi vector, *csn-5 (RNAi)* resulted in a 2.1-fold increase, and *csn-5 csn-6* double RNAi resulted in a 2.7-fold increase in UNC-98 protein. (C) Quantitative real-time PCR of *unc-98* mRNA with and without RNAi for *csn-5*. mRNA levels of *unc-98* were normalized to *ges-1*. Fold differences in mRNA levels of *unc-98* upon *csn-5 (RNAi)* were calculated relative to the empty vector, which was arbitrarily set at a value of 100. As compared with empty vector, *csn-5 (RNAi)* resulted in a 1.3-fold increase in *unc-98* mRNA levels. The graphs depict means from six experiments, and the error bars depict standard deviations.

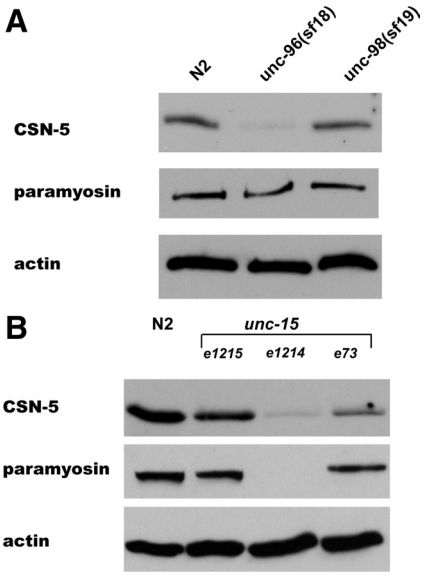

Figure 9. The effects of mutations in *unc-96*, *-98*, and *-15* on the levels of CSN-5. Extracts containing equal amounts of total Laemmli-soluble proteins from wild-type (N2), loss-of-function alleles for *unc-96 (sf18)* and *unc-98 (sf19)*, and the *unc-15* null (*e1214)* and two *unc-15* missense mutations (*e1215* and *e73*) were separated on a gel, blotted, and reacted with antibodies to the indicated proteins. (A) The level of CSN-5 protein is diminished in the *unc-96* mutant. (Paramyosin, the level of which was shown previously not to be affected in *unc-96* or *-98* and actin, serve as loading controls.) (B) The level of CSN-5 protein is significantly decreased in the paramyosin null (*e1214*), and moderately decreased in the two paramyosin missense mutants (especially *e73*).

was increased (2.1- and 2.7-fold, respectively). From the quantitative RT-PCR experiment, *csn-5 (RNAi)* resulted in a 1.3-fold increase in *unc-98* mRNA. However, because the increase in UNC-98 protein was 2.1-fold, we propose that the increase of *unc-98* mRNA is not the main reason for the increase in UNC-98 protein. Based on the interaction between UNC-98 protein and CSN-5 protein that we have demonstrated here, the known affect of the COP9 signalosome on ubiquitin-mediated proteolysis, and the lack of detectable CSN-5 protein in muscle cell nuclei, we suggest, that, at least in *C. elegans* muscle, one normal role of CSN-5 protein is to promote the degradation of UNC-98 protein. In contrast, knockdown of *csn-6*, or *csn-6* together with *csn-5* resulted in a mild decrease in UNC-96, implying that the normal function of CSN-5 is to stabilize UNC-96. Our interpretation that the normal function of CSN-5 is to promote degradation of UNC-98 is similar to most studies on the COP9 signalosome implicating a role for promoting degradation of proteins via ubiquitin-mediated proteolysis. This function for CSN-5 has also been seen in *C. elegans*, for

example, in promoting degradation of MEI-1, a katanin-like protein (Pintard *et al.*, 2003). Our results implicating a function of CSN-5 in stabilizing UNC-96, are unusual, but not unprecedented: for example, in *C. elegans*, GLH-1, a germline RNA helicase found in oocyte P granules is also stabilized by CSN-5 (Orsborn *et al.*, 2007).

It is notable that the effects of CSN-5 and -6 are different on UNC-98 and -96. Whereas *csn-5 (RNAi)* results in elevation of UNC-98 levels, it has no effect on UNC-96. In contrast, *csn-6 (RNAi)* results in no change in UNC-98 and reduced levels of UNC-96. Several studies in *Schizosaccharomyces pombe* and in *Drosophila* have shown that loss-of-function or knockdown of one CSN subunit does not always result in the same phenotype as loss-of-function or knockdown of other individual subunits, suggesting that some components may function independently from the COP9 complex (Mundt *et al.*, 2002; Oron *et al.*, 2002). Although both CSN-5 and -6 share the Mov34 domain, outside this domain there is no similarity, and thus different functions might be expected. On the other hand, it is somewhat surprising that knockdowns of either *csn-5* or *-6* have different phenotypes because *C. elegans* CSN-5 and -6 have been shown to interact by a two-hybrid assay (Pintard *et al.*, 2003), and a reconstituted human COP9 complex has been shown by a mass spectrometry approach to contain two subcomplexes, one of which has an interaction between Csn5 and Csn6 (Sharon *et al.*, 2009). Furthermore, we do not know whether the other six components of the COP9 signalosome are involved in regulating UNC-98 and -96 levels.

It has been reported that *csn-5* mRNA is expressed in both somatic and germline tissues, and is in fact, enhanced in the germline (Smith *et al.*, 2002). Two groups (Smith *et al.*, 2002 and Pintard *et al.*, 2003), using specific anti-CSN-5 antibodies, have shown that CSN-5 protein is expressed in each cell of the adult and embryo, where it is localized in the cytoplasm and also in most nuclei. Our results are the first to indicate that CSN-5 is localized to body wall muscle A-bands, and indeed the first time that any COP9 complex member has been localized to sarcomeres in any animal. Interestingly, we did not observe nuclear localization of anti-CSN-5 in body wall muscle cells.

Moreover, our results indicate that there is very high expression of *csn-5* in body wall muscle because loss-of-function mutations in *unc-96* or *-15*, genes that are primarily expressed in body wall muscle, resulted in very large decreases in the total amount of CSN-5 extracted from whole nematodes. This is surprising given that body wall muscle comprises only 95 of a total of 959 somatic cells of the worm. This high level of CSN-5 in body wall muscle is another indication that CSN-5 has an important role to play in muscle. This is an additional role for CSN-5 at least in *C. elegans*, in which it had been reported previously to be essential for oocyte development (Smith *et al.*, 2002, Pintard *et al.*, 2003). Moreover, although the COP9 signalosome has been shown in many organisms to regulate a myriad of cellular processes, ranging from cell cycle and signal transduction to transcription (Cope and Deshaies, 2003; Schwechheimer, 2004), our data are the first to show that COP9 has a role in myofibril organization and/or assembly.

Our findings also imply a novel way to regulate CSN-5: In either *unc-96* loss-of-function or *unc-15* (paramyosin) null mutants there was a substantial decrease in levels of CSN-5. This suggests that normally UNC-96 or paramyosin, by some unknown mechanism(s), indirectly promotes the expression or stabilization of CSN-5. This could occur by binding to UNC-96 or may be occurring at the transcriptional or translational levels. The possibility of transcriptional control is suggested by the large decrease in CSN-5 protein observed and that several of the proteins that UNC-96 interact with directly or indirectly are found in both myofibrils and nuclei (e.g., UNC-98, Mercer *et al.*, 2003; UNC-97, Hobert *et al.*, 1999). The stabilization of CSN-5 by paramyosin is more difficult to explain and may not occur through direct interaction of CSN-5 and paramyosin. By two-hybrid assays, full-length CSN-5 bait was tested for interaction with full-length and various deletion derivatives of paramyosin as preys. No interactions were revealed (data not shown). One possibility, however, is suggested by our previous finding that in the absence of paramyosin, the level of UNC-98 protein is reduced (Miller *et al.*, 2008); thus, less UNC-98 is available to translocate into the nucleus and stimulate transcription of target genes such as possibly, *csn-5*.

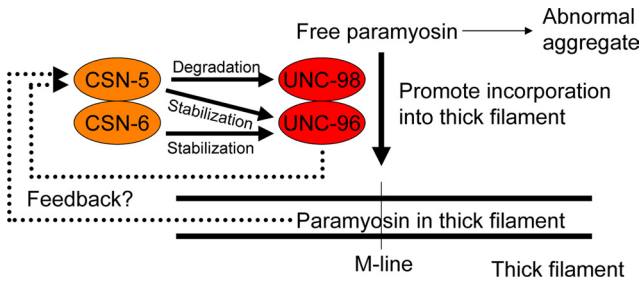

Figure 10. CSN-5 cooperates with UNC-98 and -96 to promote assembly of paramyosin into thick filaments. UNC-98 and -96 are two components of the nematode M-line and interact with each other. Paramyosin, a major component of thick filaments, is likely to exist in two pools: paramyosin incorporated into thick filaments and free paramyosin created by new synthesis or by normal turnover of thick filaments. Previous results supported a model in which UNC-98 and -96 act as chaperones to prevent abnormal aggregation of free paramyosin and thus promote its incorporation into thick filaments. In this study we show that CSN-5, a component of the COP9 signalosome, interacts with both UNC-98 and -96; that CSN-5 promotes the degradation of UNC-98 (arrow), that a combination of CSN-5 and -6 (shown by other studies to interact with each other) stabilize UNC-96 (converging arrows), and that UNC-96 and free paramyosin indirectly or through a positive feedback loop act to increase the levels of CSN-5 (dotted arrows). Overall CSN-5 and -6 act together with UNC-98 and -96 to promote the incorporation of paramyosin into thick filaments.

In our previous studies, we had shown that the birefringent needles in *unc-96* and *-98* mutants contain abnormal aggregates of paramyosin residing outside the thick filaments (Mercer *et al.*, 2006; Miller *et al.*, 2008). These needles also likely contain UNC-98 in *unc-96* mutants and UNC-96 in *unc-98* mutants (Mercer *et al.*, 2006). We can now add a fourth protein, CSN-5, by virtue of its interaction with either UNC-98 or -96 and its presence in accumulations of paramyosin in *unc-98* and *-96* mutants, as also being a component of these needles. Previously, we showed that in the absence of paramyosin, there was a decrease in UNC-98, and in the presence of abnormally aggregated paramyosin there was an increase in UNC-98. We had postulated that the dependence of UNC-98 and possibly UNC-96 levels on the state of paramyosin might be due to a chaperone function for UNC-98 or -96 to prevent aggregation of paramyosin and therefore to promote the incorporation of paramyosin into thick filaments. We can extend our model to include the regulation of UNC-98 and -96 levels (albeit in opposite directions) by CSN-5 (Figure 10).

ACKNOWLEDGMENTS

We thank Karen Bennett (University of Missouri) for supplying us some anti-CSN-5 that allowed us to first determine that CSN-5 localizes in a striated pattern in body wall muscle. We are grateful to Tsuyoshi Kawano (Tottori University) for providing us the feeding method for 2-gene RNAi. We thank Shannon McNulty for explaining to us how to quantitate Western blot results. Some strains used in this work were provided by the *Caenorhabditis* Genetics Center, which is supported by the National Center for Research Resources of the National Institutes of Health. These studies were supported by Grant AR052133 from the National Institutes of Health to G.M.B. and predoctoral fellowship 0415274B from the American Heart Association Southeast Affiliate to R.K.M.

REFERENCES

Aamodt, E. J., Chung, M. A., and McGhee, J. D. (1991). Spatial control of gut-specific gene expression during *Caenorhabditis elegans* development. Science *252*, 579–582.

Brenner, S. (1974). The genetics of *Caenorhabditis elegans*. Genetics *77*, 71–94.

Cope, G. A., and Deshaies, R. J. (2003). COP9 signalosome: multifunctional regulator of SCF and other cullin-based ubiquitin ligases. Cell *114*, 663–671.

Francis, G. R., and Waterston, R. H. (1985). Muscle organization in *C. elegans*: localization of proteins implicated in thin filament attachment an I-band organization. J. Cell Biol. *101*, 1532–1549.

Hannak, E., Oegema, K., Kirkham, M., Gonczy, P., Habermann, B., and Hyman, A. A. (2002). The kinetically dominant assembly pathway for centrosomal asters in *Caenorhabditis elegans* is gamma-tubulin dependent. J. Cell Biol. *157*, 591–602.

Hobert, O., Moerman, D. G., Clark, K. A., Beckerle, M. C., and Ruvkun, G. (1999). A conserved LIM protein that affects muscular adherens junction integrity and mechanosensory function in *C. elegans*. J. Cell Biol. *144*, 45–57.

Lin, X., Qadota, H., Moerman, D. G., and Williams B. D. (2003). *C. elegans* PAT-6/Actopaxin plays a critical role in the assembly of integrin adhesion complexes in vivo. Curr. Biol. *13*, 922–932.

Luke-Glaser, S., Roy, M., Larsen, B., Le Bihan, T., Metalnikov, P., Tyers, M., Peter, M., and Pintard, L. (2007). CIF-1, a shared subunit of the COP9/signalosome and eukaryotic initiation factor 3 complexes, regulates MEL-26 levels in the *C. elegans* embryo. Mol. Cell. Biol. *27*, 4526–4540.

Mackinnon, A. C., Qadota, H., Norman, K. R., Moerman, D. G., and Williams, B. D. (2002). *C. elegans* PAT-4/ILK functions as an adaptor protein within integrin adhesion complexes. Curr. Biol. *12*, 787–797.

Maeda, K., Nishiyama, C., Tokura, T., Nakano, H., Kanada, S., Nishiyama, M., Okumura, K., and Ogawa, H. (2006). FOG-1 represses GATA-1-dependent FcepsilonRI beta-chain transcription: transcriptional mechanism of mast-cell-specific gene expression in mice. Blood *108*, 262–269.

Mercer, K. B., Flaherty, D. B., Miller, R. K., Qadota, H., Tinley, T. L., Moerman, D. G., and Benian, G. M. (2003). *Caenorhabditis elegans* UNC-98, a C2H2 Zn finger protein, is a novel partner of UNC-97/PINCH in muscle adhesion complexes. Mol. Biol. Cell *14*, 2492–2507.

Mercer, K. B., Miller, R. K., Tinley, T. L., Sheth, S., Qadota, H., and Benian, G. M. (2006). *Caenorhabditis elegans* UNC-96 is a new component of M-lines that interacts with UNC-98 and paramyosin and is required in adult muscle for assembly and/or maintenance of thick filaments. Mol. Biol. Cell *17*, 3832–3847.

Miller, D. M., Ortiz, I., Berliner, G. C., and Epstein, H. F. (1983). Differential localization of two myosins within nematode thick filaments. Cell *34*, 477–490.

Miller, R. K., Qadota, H., Landsverk, M. L., Mercer, K. B., Epstein, H. F., and Benian, G. M. (2006). UNC-98 links an integrin-associated complex to thick filaments in *Caenorhabditis elegans* muscle. J. Cell Biol. *175*, 853–859.

Miller, R. K., Qadota, H., Mercer, K. B., Gernert, K. M., and Benian, G. M. (2008). UNC-98 and UNC-96 interact with paramyosin to promote its incorporation into thick filaments of *Caenorhabditis elegans*. Mol. Biol. Cell *19*, 1529–1539.

Moerman, D. G., and Fire, A. (1997). Muscle: structure, function and development. In: *C. elegans* II, ed. D. L. Riddle, T. Blumenthal, B. J. Meyer, and J. R. Priess, Cold Spring Harbor, NY: Cold Spring Harbor Laboratory Press, 417–470.

Moerman, D. G., and Williams, B. D. (2006). Sarcomere assembly in *C. elegans* muscle. In: WormBook, ed. The *C. elegans* Research Community, Wormbook, doi/10.1895/wormbook.1.81.1, http://www.wormbook.org.

Mundt, K. E., Liu, C., and Carr, A. M. (2002). Deletion mutants in COP9/signalosome subunits in fission yeast *Schizosaccharomyces pombe* display distinct phenotypes. Mol. Biol. Cell *13*, 493–502.

Nonet, M. L., Grundahl, K., Meyer, B. J., and Rand, J. B. (1993). Synaptic function is impaired but not eliminated in *C. elegans* mutants lacking synaptotagmin. Cell *73*, 1291–1305.

Norman, K. R., Cordes, S., Qadota, H., Rahmani, P., and Moerman, D. G. (2007). UNC-97/PINCH is involved in the assembly of integrin cell adhesion complexes in *Caenorhabditis elegans* body wall muscle. Dev. Biol. *309*, 45–55.

Oron, E., Mannervik, M., Rencus, S., Harari-Steinberg, O., Neuman-Silberberg, S., Segal, D., and Chamovitz, D. A. (2002). COP9 signalosome subunits 4 and 5 regulate multiple pleiotropic pathways in *Drosophila melanogaster*. Development *129*, 4399–4409.

Orsborn, A. M., Li, W., McEwen, T. J., Mizuno, T., Kuzmin, E., Matsumoto, K., and Bennett, K. L. (2007). GLH-1, the *C. elegans* P granule protein, is controlled by the JNK KGB-1 and by the COP9 subunit CSN-5. Development *134*, 3383–3392.

Pintard, L., Kurz, T., Glaser, S., Willis, J. H., Peter, M., and Bowerman, B. (2003). Neddylation and deneddylatin of CUL-3 is required to target MEI-1/katanin for degradation at the meiosis-to-mitosis transition in *C. elegans*. Curr. Biol. *13*, 911–921.

Qadota, H., Mercer, K. B., Miller, R. K., Kaibuchi, K., and Benian, G. M. (2007). Two LIM domain proteins and UNC-96 link UNC-97/pinch to myosin thick filaments in *Caenorhabditis elegans* muscle. Mol. Biol. Cell *18*, 4317–4326.

Qadota, H., McGaha, L. A., Mercer, K. B., Stark, T. J., Ferrara, T. M., and Benian, G. M. (2008). A novel protein phosphatase is a binding partner for the protein kinase domains of UNC-89 (obscurin) in *Caenorhabditis elegans*. Mol. Biol. Cell *19*, 2424–2432.

Schwechheimer, C. (2004). The COP9 signalosome (CSN): an evolutionary conserved proteolysis regulator in eukaryotic development. Biochem. Biophys. Acta *1695*, 45–54.

Sharon, M., Mao, H., Erba, E., Stephens, E., Zheng, N., and Robinson, C. V. (2009). Symmetrical modularity of the COP9 signalosome complex suggests its multifunctionality. Structure *17*, 31–40.

Simmer, F., Tijsterman, M., Parrish, S., Koushika, S. P., Nonet, M. L., Fire, A., Ahringer, J., and Plasterk, R.H.A. (2002). Loss of the putative RNA-directed RNA polymerase RRF-3 makes *C. elegans* hypersensitive to RNAi. Curr. Biol. *12*, 1317–1319.

Smith, P., Leung-Chiu, W-M., Montgomery, R., Orsborn, A., Kuznicki, K., Gressman-Coberly, E., Mutapcic, L., and Bennett, K. (2002). The GLH proteins, *Caenorhabditis elegans* P granule components, associate with CSN-5 and KGB-1, proteins necessary for fertility, and with ZYX-1, a predicted cytoskeletal protein. Dev. Biol. *251*, 333–347.

Timmons, L., Court, D. L., and Fire, A. (2001). Ingestion of bacterially expressed dsRNAs can produce specific and potent genetic interference in *Caenorhabditis elegans*. Gene *263*, 103–112.

Waterston, R. H. (1988). Muscle. In: The Nematode *Caenorhabditis elegans*, ed. W. B. Wood, Cold Spring Harbor, NY: Cold Spring Harbor Laboratory Press, 281–335.

Zengel, J. M., and Epstein, H. F. (1980). Identification of genetic elements associated with muscle structure in the nematode *C. elegans*. Cell Motil. *1*, 73–97.